Article

Effects of N Dilution on Laminar Burning Characteristics of Propane#Air Premixed Flames

Chenglong Tang, Zuohua Huang, Jiajia He, Chun Jin, Xibin Wang, and Haiyan Miao

Energy Fuels, **2009**, 23 (1), 151-156 • DOI: 10.1021/ef800572v • Publication Date (Web): 14 November 2008

Effects of N_2 Dilution on Laminar Burning Characteristics of Propane−Air Premixed Flames

Chenglong Tang, Zuohua Huang,* Jiajia He, Chun Jin, Xibin Wang, and Haiyan Miao

State Key Laboratory of Multiphase Flow in Power Engineering, Xi'an Jiaotong University, Xi'an 710049, People's Republic of China

Received July 19, 2008. Revised Manuscript Received October 6, 2008

Effects of nitrogen dilution on laminar burning velocities and Markstein lengths of propane−air mixtures were determined at the atmospheric pressure and room temperature based on the spherically expanding flames. The results show that, with the increase of the nitrogen dilution ratio, the burning velocity decreases and, for equivalence ratio less than 1.4, Markstein length increases with the increase of the dilution ratio, indicating that nitrogen addition decreases the preferential diffusion instability. The density ratio decreases, and the laminar flame thickness increases, which indicates the decrease of hydrodynamic instability. The ratio of unstretched laminar burning velocity with and without diluent is only related to the dilution ratio and is not influenced by the equivalence ratio. A linear correlation is found between the ratio of unstretched laminar burning velocity with and without the diluent and the dilution ratio.

1. Introduction

Increasing concern over the fossil fuel shortage and air pollution have intensified the study on alternative fuels around the world. Propane, which is a major component of liquid petroleum gas, has good air−fuel mixing potential and, hence, low HC and CO emissions because of its low boiling temperature. In addition, propane can be pressurized into the liquid stage under a moderate pressure, making onboard storage and handling easier. Widespread applications of propane, such as in furnaces, cooking stoves, water heaters, and/or fleet vehicles, are relevant to propane combustion process. Thus, the understanding of the fundamental combustion characteristics of propane flame, such as the laminar burning velocity, laminar flame thickness, the flame stability response, the ignition delay, and the flammability limits, is of particular importance and receiving increasing attention from researchers.

Laminar burning velocity is an intrinsically physiochemical property of premixed combustible gases.[1,2] Many experiments have been conducted to acquire accurate values of laminar burning velocities of premixed propane−air flames, including the stagnation plane flame method,[3,4] the heat flux method,[5,6] and the combustion bomb method.[1,7] The combustion bomb method uses the prototypical propagating spherical flame configuration and has drawn particular attention because of its simple flame configuration, well-defined flame stretch rate, and well-controlled experimentation.[8,9] Markstein length represents the sensitivity of laminar premixed flames to stretch rate, and the flame stability response is another fundamental parameter and should be studied to better understand and model the properties of laminar premixed flames.[7,10]

It is well-established that the addition of chemically passive agents or the diluents would quench the reaction zone by increased specific heats, change the transport properties, and reduce laminar burning velocities and, hence, the reaction intensity of combustible gases. However, studies of the flame stability response (represented by Markstein number) to the effects of diluent addition are still scarce. Qiao et al.[11] studied the helium-, argon-, nitrogen-, and carbon-dioxide-diluted hydrogen−oxygen premixed flames and found that, except for helium dilution, the Markstein numbers decrease with the increase of the diluent concentration, which made the flames more susceptible to preferential-diffusion instabilities. Lamoureux[12] studied hydrogen−air premixed flames with helium or carbon dioxide as diluents and found that the diluents seemed

* To whom correspondence should be addressed: State Key Laboratory of Multiphase Flow in Power Engineering, Xi'an Jiaotong University, Xi'an 710049, People's Republic of China. E-mail: zhhuang@mail.xjtu.edu.cn.

(1) Marley, S. K.; Roberts, W. L. Measurements of laminar burning velocity and Markstein number using high-speed chemiluminescence imaging. *Combust. Flame* **2005**, *141* (4), 473–477.

(2) Law, C. K.; Sung, C. J. Structure, aerodynamics, and geometry of premixed flamelets. *Prog. Energy Combust. Sci.* **2000**, *26* (4−6), 459–505.

(3) Yu, G.; Law, C. K.; Wu, C. K. Laminar flame speeds of hydrocarbon + air mixtures with hydrogen addition. *Combust. Flame* **1986**, *63* (3), 339–347.

(4) Vagelopoulos, C. M.; Egolfopoulos, F. N. Direct experimental determination of laminar flame speeds. *Int. Symp. Combust.* **1998**, *27* (1), 513–519.

(5) Bosschaart, K. J.; de Goey, L. P. H.; Burgers, J. M. The laminar burning velocity of flames propagating in mixtures of hydrocarbons and air measured with the heat flux method. *Combust. Flame* **2004**, *136* (3), 261–269.

(6) Bosschaart, K. J.; de Goey, L. P. H. Detailed analysis of the heat flux method for measuring burning velocities. *Combust. Flame* **2003**, *132* (1−2), 170–180.

(7) Tseng, L. K.; Ismail, M. A.; Faeth, G. M. Laminar burning velocities and Markstein numbers of hydrocarbon/air flames. *Combust. Flame* **1993**, *95* (4), 410–426.

(8) Bradley, D.; Gaskell, P. H.; Gu, X. J. Burning velocities, markstein lengths, and flame quenching for spherical methane−air flames: A computational study. *Combust. Flame* **1996**, *104* (1−2), 176–198.

(9) Sun, C. J.; Sung, C. J.; He, L.; Law, C. K. Dynamics of weakly stretched flames: Quantitative description and extraction of global flame parameters. *Combust. Flame* **1999**, *118* (1−2), 108–128.

(10) Kwon, S.; Tseng, L. K.; Faeth, G. M. Laminar burning velocities and transition to unstable flames in $H_2/O_2/N_2$ and $C_3H_8/O_2/N_2$ mixtures. *Combust. Flame* **1992**, *90* (3−4), 230–246.

(11) Qiao, L.; Kim, C. H.; Faeth, G. M. Suppression effects of diluents on laminar premixed hydrogen/oxygen/nitrogen flames. *Combust. Flame* **2005**, *143* (1−2), 79–96.

(12) Lamoureux, N.; Djebaili-Chaumeix, N.; Paillard, C. E. Laminar flame velocity determination for H_2−air−He−CO_2 mixtures using the spherical bomb method. *Exp. Therm. Fluid Sci.* **2003**, *27* (4), 385–393.

10.1021/ef800572v CCC: $40.75
Published on Web 11/14/2008

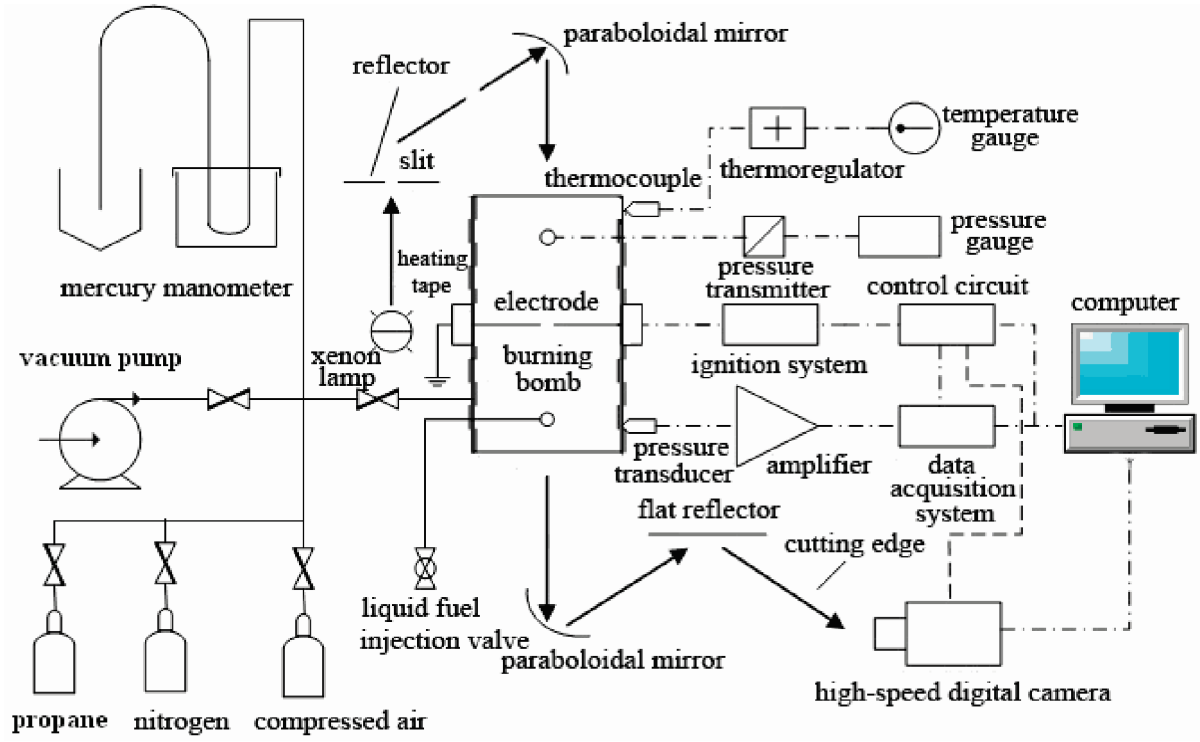

Figure 1. Experimental setup.

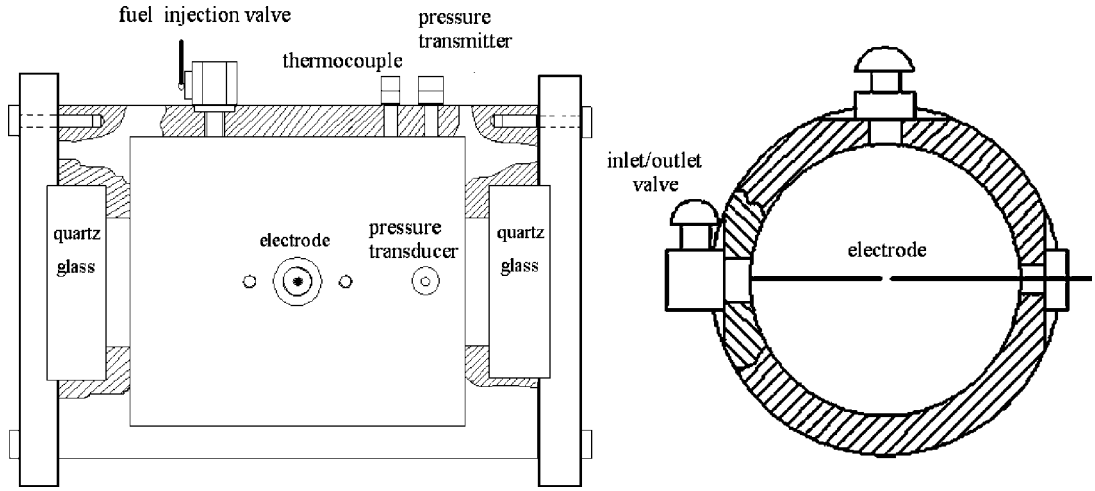

Figure 2. Combustion vessel.

not to affect Markstein numbers. Kwon[13] studied nitrogen-, argon-, or helium-diluted hydrogen−oxygen flames and found that both nitrogen and argon decreased Markstein numbers slightly, indicating their destabilizing effect, and their effects were almost the same because of their similar transport properties, while helium dilution increased Markstein numbers, indicating a stabilizing effect because the increased thermal diffusivity overweighed the increase of mass diffusivity. Aung et al.[14] studied nitrogen-diluted hydrogen−air flame and stated that the values of Markstein numbers were relatively independent of nitrogen dilution. The limited literature of dilution effects on flame stability response is mostly for hydrogen−air flames. Propane−air and hydrogen−air flames have opposite non-equidiffusive behavior for the lean and rich flames; thus, the study on the dilution effect on flame stability response of the propane−air mixture is important.

Because the highest concentration of most combustion exhaust gas is nitrogen and, in addition, nitrogen is an easily available and cost-effective candidate as a diluent, in this paper, nitrogen is chosen to study the effect of dilution on laminar burning characteristics of propane−air mixtures with the outwardly propagating spherical flame and the high-speed schlieren photography.

2. Experimental Setup and Procedures

In this work, the dilution ratio is defined as the volumetric fraction of nitrogen addition in the premixtures

$$\phi_r = \frac{V_{diluent}}{V_{fuel} + V_{air} + V_{diluent}} \quad (1)$$

As shown in Figure 1, the experimental apparatus consists of the combustion vessel, the heating system, the ignition system, the

(13) Kwon, O. C.; Faeth, G. M. Flame/stretch interactions of premixed hydrogen-fueled flames: Measurements and predictions. *Combust. Flame* **2001**, *124* (4), 590–610.

(14) Aung, K. T.; Hassan, M. I.; Faeth, G. M. Effects of pressure and nitrogen dilution on flame/stretch interactions of laminar premixed $H_2/O_2/N_2$ flames. *Combust. Flame* **1998**, *112* (1−2), 1–15.

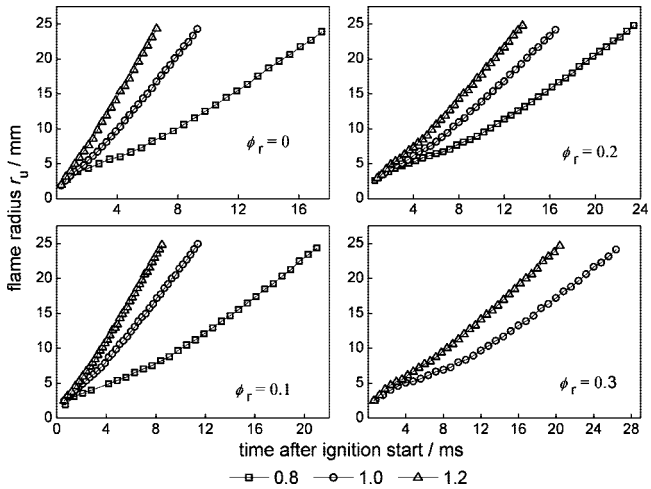

Figure 3. Flame radius versus time.

data acquisition system, and the high-speed schlieren photography system. Figure 2 shows the schematic diagram of the cylinder-type combustion vessel with a diameter of 180 mm and length of 210 mm. Two sides of the vessel are mounted with the quartz windows to allow for optical access. A high-speed digital camera operating at 10 000 frames per second was used to record the flame pictures during the flame propagation. A Kistler pressure transducer was used to record the combustion pressure. The mixtures were prepared by introducing each component according to its corresponding partial pressure for the specified overall equivalence ratio. The mixtures are ignited by the centrally located electrodes. A standard capacitive discharge ignition system is used to produce the spark. Once the combustion was completed, the combustion vessel was vacuumed and flushed with dry air 3 times to avoid the influence of the residual gas on the next experiment. A time interval of 5 min was adopted to allow the mixtures to be quiescent and to avoid the influence of wall temperature. A time interval of 30 min was tested, and no appreciable difference was observed compared to the time interval of 5 min. As the flame develops in a spherical pattern, the flame radius is scaled from the flame photo recorded by the high-speed camera.

The flame propagation speed, S_n, is the velocity of the flame front relative to a fixed position, the combustion vessel wall, for instance. For outwardly propagating flames, S_n is derived from the flame radius−time history[8,15,16] as

$$S_n = \frac{dr_u}{dt} \tag{2}$$

where r_u is the flame radius in schlieren photographs and t is the elapsed time from ignition.

Flame stretch rate, α, is defined as the derivative of the logarithm of the flame front area A with respect to time, that is

$$\alpha = \frac{d(\ln A)}{dt} = \frac{1}{A}\frac{dA}{dt} \tag{3}$$

For outwardly propagating flames, the above equation could be simplified as

$$\alpha = \frac{1}{A}\frac{dA}{dt} = \frac{2}{r_u}\frac{dr_u}{dt} = \frac{2}{r_u}S_n \tag{4}$$

In the early stage of flame propagation, a linear relationship exists between the flame propagation speed and the stretch rate

$$S_l - S_n = L_b\alpha \tag{5}$$

where S_l is the unstretched propagation speed derived from extrapolating S_n to zero stretch rate and L_b is the burned gas Markstein length, which represents the sensitivity of the flame stability response to the stretch rate. A positive value of L_b indicates that the flame speed decreases with the increase of the flame stretch rate; in this case, the protuberance of the flame front is suppressed and the flame tends to be stable. In contrast, a negative value of L_b means that the flame speed increases with the increase of the flame stretch rate; in this case, any protuberance of the flame front will be promoted because of a local flame speed increase and the flame tends to be unstable.[15,17] Actually, three factors contribute to the flame instability of the premixed laminar flames, namely, the body force effect, the hydrodynamic effect, and the thermal diffusive effect.[11,18] The body force or the buoyancy, in other words, affects the flame instability only near flammability limits when the burning velocities are very low and is detected by mushroom-shaped flames. Hydrodynamic instability could be identified by the development of a somewhat regular cellular disturbance pattern on the flame surface, and this instability is promoted by the increase in the density ratio across the flame and the decrease in flame thickness.[19,20] Fortunately, this instability is only observed when the flame radii are large enough where the curvature induced stretch can no longer suppress the cellular instability. Preferential diffusion instability is observed only when the Markstein number or Markstein length is negative and could be identified by irregular (chaotic) distortions of the flame surface relatively early in the flame propagation process. Fortunately, flame surfaces remained smooth at small flame radii even for conditions that involved preferential-diffusion instability, and the laminar burning velocities could be

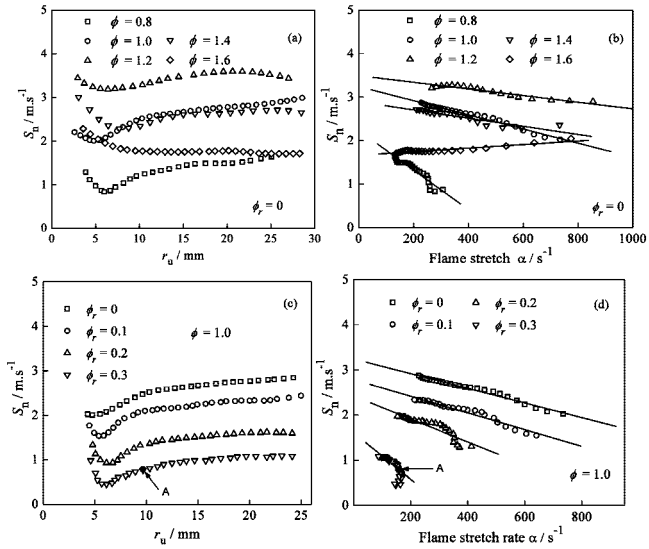

Figure 4. Flame propagation speed versus the flame radius and stretch rate.

(15) Huang, Z.; Zhang, Y.; Zeng, K.; Liu, B.; Wang, Q.; Jiang, D. Measurements of laminar burning velocities for natural gas−hydrogen−air mixtures. *Combust. Flame* **2006**, *146* (1−2), 302–311.

(16) Bradley, D.; Hicks, R. A.; Lawes, M.; Sheppard, C. G. W.; Woolley, R. The measurement of laminar burning velocities and Markstein numbers for iso-octane−air and iso-octane−*n*-heptane−air mixtures at elevated temperatures and pressures in an explosion bomb. *Combust. Flame* **1998**, *115* (1−2), 126–144.

(17) Huang, Z.; Wang, Q.; Yu, J.; Zhang, Y.; Zeng, K.; Miao, H.; Jiang, D. Measurement of laminar burning velocity of dimethyl ether−air premixed mixtures. *Fuel* **2007**, *86* (15), 2360–2366.

(18) Clavin, P. Dynamic behavior of premixed flame fronts in laminar and turbulent flows. *Prog. Energy Combust. Sci.* **1985**, *11* (1), 1–59.

(19) Kwon, O. C.; Rozenchan, G.; Law, C. K. Cellular instabilities and self-acceleration of outwardly propagating spherical flames. *Proc. Combust. Inst.* **2002**, *29* (2), 1775–1783.

(20) Jomaas, G.; Law, C. K.; Bechtold, J. K. On transition to cellularity in expanding spherical flames. *J. Fluid Mech.* **2007**, *583*, 1–26.

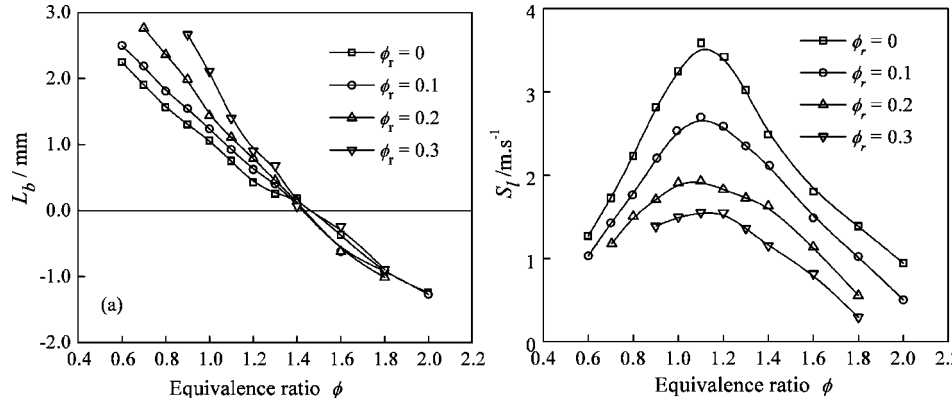

Figure 5. L_b and S_l versus the equivalence ratio at different dilution ratios.

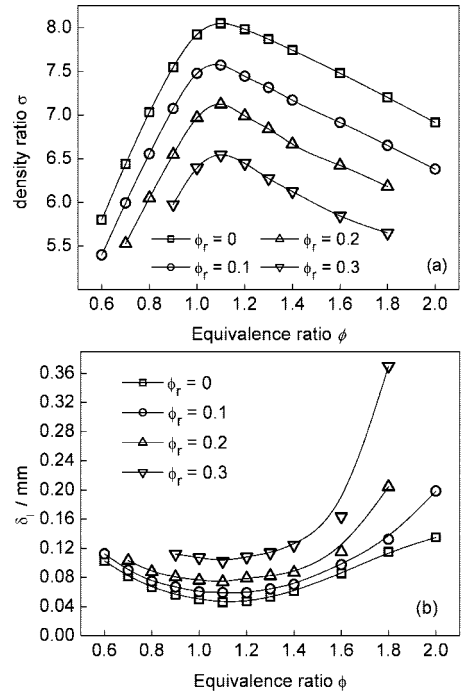

Figure 6. Density ratio and flame thickness versus the equivalence ratio.

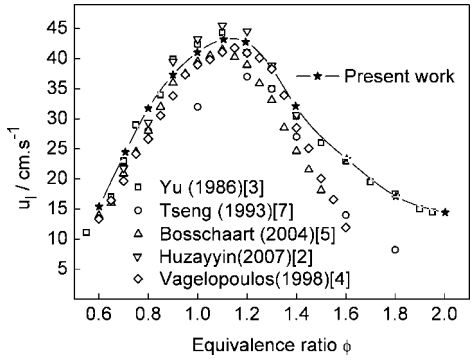

Figure 7. Comparisons of experimental data u_l with different literature.

measured for a time even at these conditions. In this paper, measurements were limited in the early stage of flame propagation, where the flame radii were smaller than 25 mm and all of the flame pictures were well-spherical; therefore, only the preferential diffusion instability is discussed. Markstein,[21] Manton,[22] and Parlange[23]

(21) Markstein, G. H. Cell structure of propane flames burning in tubes. *J. Chem. Phys.* **1949**, *17* (4), 428–429.

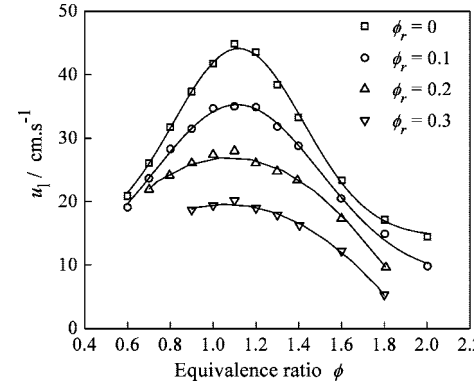

Figure 8. u_l versus the equivalence ratio at different dilution ratios.

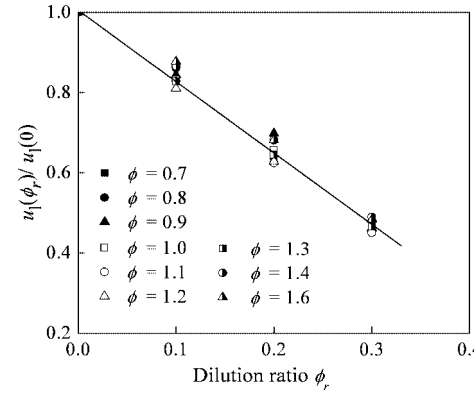

Figure 9. $u_l(\phi_r)/u_l(0)$ versus the dilution ratio at different equivalence ratios.

Table 1. Summary of Experimental Conditions

initial pressure = 0.1 MPa	initial temperature = 300 K
dilution ratio (%)	fuel equivalence ratio
0	0.6, 0.7, 0.8, 0.9, 1.0, 1.1, 1.2, 1.3, 1.4, 1.6, 1.8, 2.0
10	0.6, 0.7, 0.8, 0.9, 1.0, 1.1, 1.2, 1.3, 1.4, 1.6, 1.8, 2.0
20	0.7, 0.8, 0.9, 1.0, 1.1, 1.2, 1.3, 1.4, 1.6, 1.8
30	0.9, 1.0, 1.1, 1.2, 1.3, 1.4, 1.6, 1.8

showed that the flame tends to be stable because of the preferential diffusion effect if the more rapidly diffusing constituent is present in excess. According to their theory, if heavy hydrocarbon−air mixtures are below stoichiometry, the flames are stable to the preferential diffusion effect ($L_b > 0$); in contrast, the flames are

(22) Manton, J.; von Elbe, G.; Lewis, B. Nonisotropic propagation of combustion waves in explosive gas mixtures and the development of cellular flames. *J. Chem. Phys.* **1952**, *20* (1), 153–157.

(23) Parlange, J. Y. Influence of preferential diffusion on the stability of a laminar flame. *J. Chem. Phys.* **1968**, *48* (4), 1843–1849.

unstable to the preferential diffusion effect ($L_b < 0$) if heavy hydrocarbon−air mixtures are over stoichiometry. At stoichiometric condition, L_b tends to be zero.

On the early stage of flame propagation, the flame undergoes an isobaric developing process and the unstretched laminar burning velocity u_l is related to S_l according to mass conservation across the flame front

$$A_f\rho_u u_l = A_f\rho_b S_l \quad (6)$$

where A_f is the flame front area and ρ_u and ρ_b are density of unburned and burned gas, respectively. u_l is deduced from eq 6 as follows:

$$u_l = \rho_b S_l/\rho_u \quad (7)$$

In this study, the laminar flame thickness δ_l is determined with the suggestion of Law et al.[2,24]

$$\delta_l = (\lambda/C_p)/(\rho_u u_l) \quad (8)$$

3. Results and Discussion

3.1. Flame Propagation Speeds and Markstein Lengths. In the experiment, the combustible mixtures were spark-ignited. For outwardly premixed flames, the propagation speed becomes independent of the igniting energy for radii greater than 6 mm.[8] In this paper, data processing was limited for flame radii larger than 6 mm and smaller than 25 mm.

Figure 3 illustrates flame radii (r_u) development at equivalence ratios $\phi = 0.8$, 1.0, and 1.2 for different dilution ratios. The flame radius increases monotonically with the time. A linear relationship existed between the flame radius and time, except at the initial stage of flame development, where the influence of ignition energy and electrode cooling is apparent, and the behavior is more obvious for the lean mixture and high dilution ratio combustion, where the flame speed is relatively low. With the increase of the dilution ratio, the flame develops more slowly.

Figure 4a gives the propagation speed of propane−air mixtures versus the flame radius for various equivalence ratios. At the very early stage (r_u less than about 6 mm), the flame propagation speed decreases significantly with the increase of the flame radius because of the initial spark energy influence and the subsequent electrode cooling effect. For flame radii larger than 6 mm, the flame propagation speed generally increases with the increase of the flame radius for equivalence ratios $\phi < 1.4$, while decreasing slightly with the increase of the flame radius for $\phi > 1.4$. Figure 4b gives the flame propagation speed versus the flame stretch rate for various equivalence ratios. There exists a linear relationship between the propagation speed (S_n) and the flame stretch rate (α) for various equivalence ratios. The slope of $S_n-\alpha$ linear fit is negative for $\phi < 1.4$ and positive for $\phi > 1.4$, indicating a positive and negative value of Markstein length (L_b) for equivalence ratios smaller and larger than 1.4, respectively. Parts c and d of Figure 4 illustrate the flame propagation speed versus flame radius and stretch rate at $\phi = 1.0$ for different dilution ratios (ϕ_r). It is clear that diluent addition decreases the propagation speed significantly. Furthermore, for $\phi_r = 0.3$, at high stretch rate (small radius), the sharp fall in S_n with the stretch rate at point A indicates that, in this regime, a fully developed flame is not yet established. This behavior is quite similar to that observed by Bradley et al.[16] for iso-octane−air flame and by Huang et al.[15] for natural gas−air flame, and data in this regime are not used for linear regression.

Parts a and b of Figure 5 give the Markstein lengths (L_b) and unstretched propagation speeds (S_l) derived from eq 5. It can be seem from Figure 5a that L_b decreases from positive to negative with the increase of the equivalence ratio and, at the equivalence ratio of 1.4, L_b equals zero. For $\phi < 1.4$ cases, L_b is positive and L_b increases with the increase of the dilution ratio, indicating the stabilizing effect of nitrogen addition. In this case, the propane−air flames are intrinsically stable based on the classical model of Markstein[21] and Manton;[22] namely, laminar premixed flames are stable to effects of preferential diffusion at conditions where the fast diffusing component (air) is present in abundance. The addition of nitrogen makes the fast diffusing component relatively more abundant and the flames more stable to the preferential diffusion effect, and thus, the Markstein lengths are shifted toward more positive (stable) values. In contrast, for $\phi > 1.4$ cases, the influence of nitrogen addition is moderated. In these cases, it is seen that nitrogen suppression has little effect on either the trends or magnitudes of L_b, even though nitrogen addition would decrease the flame temperature significantly because of decreased heat release and increased specific heat. This is because, for $\phi > 1.4$, the faster diffusion component (air) is deficient and the flames are unstable to preferential diffusion effects. In addition, nitrogen has similar transport properties as that of oxygen. The equivalence ratio of which L_b equals zero is important because, in this case, the flame speed is least affected by the flame stretch rate. Marley[1] and Tseng[7] obtained this value in their research, which were 1.34 and 1.44, respectively. In the present work, this value is approximately 1.4, regardless of the dilution ratios. Figure 5b illustrates the suppression effect of nitrogen addition on the unstretched flame propagation speed. It can be drawn that nitrogen addition decreases the unstretched flame propagation speed significantly for various equivalence ratios, and this effect is the most apparent at the equivalence ratio of 1.1, at which the unstretched propagation speed reaches its maximum value.

3.2. Laminar Burning Velocity. Parts a and b of Figure 6 give the density ratio (σ) and the laminar flame thickness (δ_l) versus the equivalence ratio for various dilution ratios. σ and δ_l decreases and increases, respectively, as the mixture becomes more off-stoichiometric. With the increase of the dilution ratio, σ is decreased and δ_l is increased, and this indicates that the hydrodynamic instability is suppressed with the increase of the nitrogen dilution ratio.

Figure 7 gives the unstretched laminar burning velocity for the propane−air mixture of the present study, and some literature values are presented for comparison. The present work agrees best with that by Yu et al.,[3] with the symmetrical, adiabatic, counterflow arrangement and involved the consideration of the heat loss and the stretch effect. The result of the heat flux method by Bosschaart et al.[5] gives lower values than most of the other measurements, as suggested in ref 5. At fuel-rich conditions, the result of Vagelopoulos et al.[4] with the single jet-plate configuration is lower than the present study. This may be caused by the slower flame propagation at fuel-rich conditions and the correspondingly larger downstream heat loss. Tseng[7] used the outwardly propagating spherical flame configuration as the same in the present work. However, the maximum values of laminar burning velocities seem to be shifted toward larger fuel equivalence ratios. Huzayyin[25] used the pressure−time

(24) Law, C. K.; Jomaas, G.; Bechtold, J. K. Cellular instabilities of expanding hydrogen/propane spherical flames at elevated pressures: Theory and experiment. *Proc. Combust. Inst.* **2005**, *30* (1), 159–167.

(25) Huzayyin, A. S.; Moneib, H. A.; Shehatta, M. S.; Attia, A. M. A. Laminar burning velocity and explosion index of LPG−air and propane−air mixtures. *Fuel* **2007**, *87* (1), 39–57.

history and many combustion models to obtain the laminar burning velocity, and here, only the results of Manton's model as a representative is presented. It is well-known that the pressure−time approach disregards the effect of the flame stretch and turbulence, and this leads to the higher values of laminar burning velocity near stoichiometric conditions.

Figure 8 gives the unstretched laminar burning velocity versus the equivalence ratio for various dilution ratios. For the four dilution ratios studied herein, the unstretched laminar burning velocity u_l exhibits the parabola-like variation with respect to the equivalence ratio. For a given equivalence ratio, u_l decreases with the increase of the dilution ratio as a result of the diluent per unit oxygen concentration. This causes a corresponding reduction in temperature within the reaction zone of the flames with the associated reduction of laminar burning velocities.

The ratio of the unstretched laminar burning velocity with and without nitrogen dilution is plotted in Figure 9. For all equivalence ratios, there exists a linear correlation between $u_l(\phi_r)/u_l(0)$ and ϕ_r. For a specified ϕ_r, $u_l(\phi_r)/u_l(0)$ almost gives the same value regardless of the equivalence ratio, and this reflects the fact that the mixture dilution has the same influence to u_l of the propane−air−diluent mixtures under all equivalence ratios. On the basis of the experimental data, the following correlation is proposed:

$$\frac{u_l(\phi_r)}{u_l(0)} = A\phi_r + B \tag{9}$$

where $A = -1.84$ and $B = 1.0$.

4. Conclusions

Effects of nitrogen dilution on laminar burning velocity and Markstein length are studied. The main results are summarized as follows: (1) For nitrogen-diluted propane−air mixtures, both the laminar propagation speed and laminar burning velocity decrease dramatically with the increase of the dilution ratio. Markstein length increases with the increase of the dilution ratio for equivalence ratios smaller than 1.4, indicating that nitrogen addition decreases preferential diffusion instability. The density ratio decreases and the flame thickness increases with the increase of the dilution ratio, and this indicates the decrease of hydrodynamic instability. (2) The ratio of unstretched laminar burning velocities with and without nitrogen addition is linearly related to the dilution ratio and is not influenced by the equivalence ratio.

Acknowledgment. The study is supported by the National Natural Science Foundation of China (50636040 and 50521604) and the National Basic Research Program (2007CB210006).

Nomenclature

A_f = flame area
ρ_b = density of burned gas
ρ_u = density of unburned gas
S_l = unstretched flame propagation speed
S_n = stretched flame propagation speed
t = time
u_l = unstretched laminar burning velocity
L_b = burned gas Markstein length (mm)
r_u = flame radius
σ = density ratio (ρ_u/ρ_b)
ϕ = fuel equivalence ratio
ϕ_r = nitrogen dilution ratio
α = flame stretch rate
δ_l = laminar flame thickness (mm)

EF800572V